

APVR: Hour-Level Long Video Understanding with Adaptive Pivot Visual Information Retrieval

Hong Gao^{1,2*}, Yiming Bao^{2*}, Xuezhen Tu², Bin Zhong², Minling Zhang^{1†}

¹SouthEast University, ²ZTE Corporation

Abstract

Current multimodal large language models (MLLMs) struggle with hour-level video understanding, facing significant challenges not only in modeling the substantial information volume of long videos but also in overcoming the memory wall and resource constraints during both training and inference. Although recent training-free approaches have alleviated resource demands by compressing visual features, their reliance on incomplete visual information limits the performance potential. To address these limitations, we propose **Adaptive Pivot Visual information Retrieval (APVR)**, a training-free framework that hierarchically retrieves and retains sufficient and important visual information. It breakthroughs the memory wall limitation via two complementary components: Pivot Frame Retrieval employs query expansion and iterative spatio-semantic confidence scoring to identify relevant video frames, and Pivot Token Retrieval performs query-aware attention-driven token selection within up to 1024 pivot frames. This dual granularity approach enables the processing of hour-long videos while maintaining semantic fidelity. Experimental validations demonstrate significant performance improvements, achieving 64.9% on LongVideoBench and 68.4% on VideoMME, which are state-of-the-art results for both training-free and training-based approaches. Meanwhile, our method provides plug-and-play integration capability with existing MLLM architectures.

1 Introduction

The proliferation of long-form video content necessitates robust understanding capabilities that extend beyond the current limitations of multimodal large language models (MLLMs). While existing video-based models (Lin et al. 2023; Zhang et al. 2025) demonstrate proficiency on short video sequences, their scalability for hour-level video remains challenging. Specifically, they encounter not only the memory wall but also the inherent dilution of semantic information across extensive temporal spans.

The core challenge stems from the inability of current Video MLLMs to effectively model and extract critical information from long video sequences. In hour-level videos, semantically relevant contents are typically sparse across both temporal and spatial dimensions. However, existing

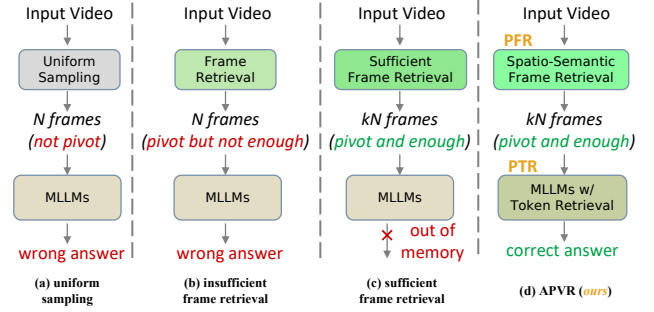


Figure 1: Given a long video, uniform sampling (a) and insufficient frame retrieval (b) yield incorrect answer, while naively increasing pivot frames (c) raises OOM. Our APVR (d) explores joint frame-token co-retrieval, concentrating computational resources on the most relevant information.

approaches process entire sequences by uniform sampling, leading to computational inefficiency and degraded performance due to attention dispersion across irrelevant segments. As illustrated in Fig. 1(a), this strategy samples frames that are not pivot, leading to wrong answer generated by MLLMs.

Recently, some approaches (Ataallah et al. 2024; Tang et al. 2025a; Guo et al. 2025; Ye et al. 2025; Cheng et al. 2025; Luo et al. 2025) have attempted to retrieve query-relevant frames from long videos, simplifying long video understanding task as key-frame selection. Consequently, MLLMs process only few and sparse key frames instead of continuous video frames, neglecting the temporal-semantic relationships and potentially failing in scenarios requiring comprehensive temporal reasoning and long-range logical understanding, as shown in Fig. 1(b).

A potential solution to the above limitation is to retrieve sufficient pivot frames and improve coverage as shown in Fig. 1(c). However, such approaches encounter the memory wall when processing these frames with MLLMs. While recent training-based methods employ strategies such as multimodal sequence parallelism (Fu et al. 2025; Liu et al. 2024d) or feature compression (Shu et al. 2024; Liu et al. 2025a) during the training phase to accommodate extended video frames, they demand resource-intensive multi-stage training based on existing MLLMs. Thus, they lack adaptability to rapidly evolving MLLM architectures due to high

*Equal Contribution

†Corresponding Author

retraining costs.

The inherent trade-off between temporal coverage and computational feasibility has hindered existing methods from achieving comprehensive video understanding. To address this core challenge, we propose **Adaptive Pivot Visual information Retrieval (APVR)** framework, a training-free approach that integrates spatio-semantic frame retrieval with token retrieval and compression, as shown in Fig. 1(d). This two-stage retrieval mechanism enables the system to concentrate computational resources on the pivot visual information that is most relevant to the input query, thus efficiently processing hour-long videos without encountering memory limitations.

Specifically, at the frame level, our *Pivot Frame Retrieval (PFR)* component expands the original query into four types of semantic information: *objects*, *descriptions*, *relations*, and *semantics*. This expansion enables more comprehensive frame scoring from spatial and semantic perspectives using complementary visual models: CLIP for semantic similarity and Grounding-DINO for object detection and spatial reasoning. The framework incorporates temporal diffusion mechanisms to maintain temporal coherence and employs adaptive resampling strategies to progressively refine frame selection across multiple iterations. At the token level, our *Pivot Token Retrieval (PTR)* component extends the concept of semantic importance to fine-grained visual representations. This component leverages query-aware multi-layer attention scoring to identify the most relevant visual tokens within selected frames, employing dynamic chunk-wise selection and head-wise soft voting mechanisms to maintain both computational efficiency and semantic accuracy.

The main contributions of this work are summarized as follows:

- We propose APVR, a novel training-free framework that addresses scalability challenges in long video understanding through dual-granularity information retrieval. Our approach combines frame-level pivot retrieval with token-level adaptive selection to breakthrough the memory wall.
- We develop a mechanism that leverages spatio-semantic confidence scoring and query-aware attention scoring to preserve temporal structure and semantic details, ensuring accurate understanding of complex video narratives while maintaining computational efficiency.
- We demonstrate that intelligent dual-granularity retrieval provides a sustainable alternative to parameter scaling for long video understanding. Our training-free design ensures plug-and-play integration with existing MLLM architectures while preserving foundational capabilities.

2 Related Work

Video MLLMs Recent years have witnessed significant advances in multimodal large language models (MLLMs) for visual perception and understanding. As a critical modality in visual data analysis, video has also been integrated into MLLM frameworks. Notable efforts include Qwen2.5-VL (Bai et al. 2025a), InternVideo2.5 (Wang et al. 2025b), VideoLlama3 (Zhang et al. 2025), and VideoChat-Flash (Li et al. 2024b), which explore video understanding through a

unified architecture consisting of three key components: (a) a video encoder for spatio-temporal feature extraction, (b) a projector for aligning visual features with linguistic embeddings, and (c) a video-aware LLM for multimodal reasoning. Due to the inherent complexity of video content (e.g., multi-object interactions, long-range temporal dependencies), existing MLLMs often fail to extract semantically salient information for video-centric downstream tasks requiring precise spatiotemporal reasoning, such as video question answering and spatiotemporal video grounding. Some works (Bai et al. 2025a; Wei et al. 2025) exploit to aggregate timestamps in the RoPE (Su et al. 2024). However, these methods exhibit significant performance degradation when extrapolating to videos exceeding their pre-training duration. Moreover, current architectures also exhibit limitations of inefficient cross-modal alignment between visual information and linguistic queries, particularly in long-form videos exceeding 5 minutes (Li et al. 2024a).

Long Video Understanding Recently advances in long video understanding can be broadly categorized into training-based and training-free paradigms. In the training-based paradigm, MLLMs are directly trained using large-scale long video datasets. The whole training process is usually divided into several stages to stably improve different components of MLLM, as well as to improve the ability to model different types of input visual data (Li et al. 2024b; Zhang et al. 2025). In order to process extra-long videos, current methods explore two different strategies: sequence parallelism (Chen et al. 2024; Zhang et al. 2024b; Shen et al. 2025) or visual feature compression (Song et al. 2024; Shen et al. 2024; Liu et al. 2025a). For instance, LongVILA (Chen et al. 2024) adopts a five-stage training pipeline with a novel multi-modal sequence parallelism to efficiently understand long videos. Video-XL-Pro (Liu et al. 2025a) builds a learnable module to generate compact and comprehensive video tokens for hour-long video understanding. In the training-free paradigm, long video understanding task is organized as an agent-like process (Liu et al. 2025b; Wang et al. 2024c), where MLLMs serve as reasoning engine within the system. These training-free methods mainly focus on retrieving the most important information in video frames (Tang et al. 2025b; Park et al. 2024; Ye et al. 2025; Guo et al. 2025; Cheng et al. 2025) or visual tokens (Wang et al. 2025a; Luo et al. 2025). For example, AKS (Tang et al. 2025b) adopts a plug-and-play module for keyframe selection and information pre-filtering for video-based MLLMs. QuoTA (Luo et al. 2025) adopts an ante-hoc training-free modular for query-aware visual token assignment and important information retrieval. Despite these advancements, few methods simultaneously explore frame and token optimization, which is addressed in this work through adaptive pivot information retrieval.

3 Method

3.1 Overview

The framework of the proposed APVR is illustrated in Fig. 2, which is a training-free system. Given an input video $\mathcal{F} = \{f_t\}_{t=1}^N$ with N frames sampled under specific fps

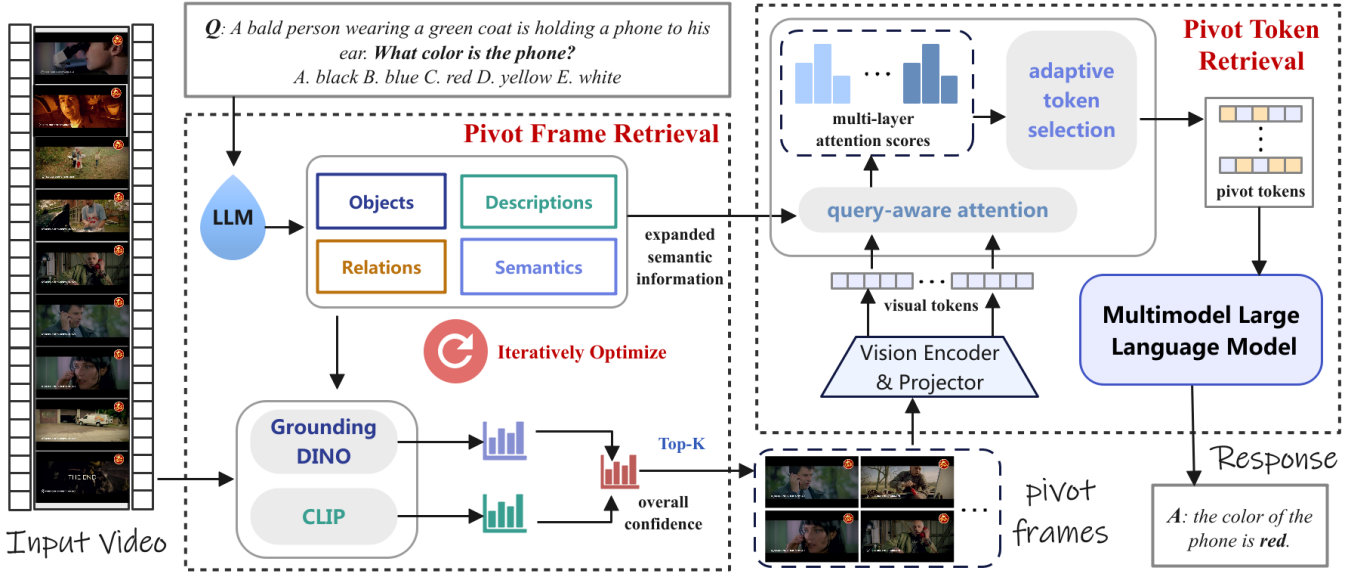


Figure 2: The overall framework of our proposed APVR. We integrate two plug-and-play components, Pivot Frame Retrieval and Pivot Token Retrieval, into MLLMs to improve the performance of long video understanding. APVR is training-free and provides a alternative to parameter scaling. With frame-level and token-level adaptive selection, it can accurately understand complex videos with computational efficiency.

and query Q , the system aims to retrieve the most important visual information for accurate response. To achieve this, we build two main components in APVR: *Pivot Frame Retrieval* (PFR) and *Pivot Token Retrieval* (PTF). In PFR, we search pivot frames \mathcal{F}_{pivot} with high confidence scores using expanded queries and basic visual models. In PTR, we explore an attention-driven token selection in MLLMs to retrieve pivot tokens \mathcal{T}_{pivot} that are most relevant with expanded queries.

3.2 Pivot Frame Retrieval

The progress of PFR is developed in an iterative and efficient manner, as elaborated in Alg. 1.

Semantic Information Expansion First, We expand the given query Q to four types of semantic information as follows:

Objects: The key objects Obj_k or cue objects Obj_c that are detectable by visual models such as Grounding-DINO (e.g., “bold person”, “phone”, “blue background”). All objects are aggregated as $Obj = \{Obj_k, Obj_c\}$.

Descriptions: The entities or hypernym concepts of objects based on knowledge graph augmentation, denoted as Des . (e.g. “pearl headband: decorative accessory worn on head; jewelry”)

Relations: The triplet relationship $Rel \subseteq Obj \times \mathcal{R} \times Obj$ to enhance the confidence of frames with logical links between objects. In each triplet (o_i, r, o_j) , the type of relation $r \in \mathcal{R}$ is exactly one of the following: (1) **spatial** which means that o_i and o_j appear in the same frame, such as “a bold man holding a red phone”. (2) **time** which means that o_i and o_j appear in different frames in orders such as “A woman walks through, after a cat follows.” (3) **attribute** which means that

o_i appears with an attribute describable by o_j such as “A woman in a white skirt”. (4) **causal** which means that o_i and o_j appear in orders with a cause-effect manner such as “A woman opens the door, the cat is scared and runs out.”

Semantics: The semantics information of query and options based on knowledge graph, denoted as Sem (e.g., ‘leash often appears with dog”).

The prompt template for LLM-based query expansion is provided in Appendix.

Spatio-Semantic Confidence Scoring Given a video \mathcal{F} , and query Q with expanded semantic information $\{Obj, Des, Rel, Sem\}$, instead of exhaustively processing all N frames, we uniformly sample few frames with initial stride ∇ in the first iteration and adaptively resample frames for the subsequent iteration based on the online updated frame confidence. To ensure progressively finer sampling, we gradually decrease the stride by $\nabla^p = \max(1, \frac{\nabla}{p})$. The frames sampled in iteration p are denoted as \mathcal{F}_{smp}^p .

Our algorithm exploits two basic visual models, i.e., Grounding-DINO and CLIP, to comprehensively score \mathcal{F}_{smp}^p as follows:

CLIP-based Similarity Scoring: We leverage the CLIP model to compute cross-modal similarity between text and visual features as the semantic confidence score based on expanded query and the visual feature by $s_t^{CLIP} = \Pi_{CLIP}(f_t, Q, Des, Sem)$. The details of the function Π_{CLIP} are provided in Appendix.

Grounding-DINO Object Detection: We leverage the Grounding-DINO model to compute the spatial confidence score based on the query-aware objects long with their relations by $s_t^{GD} = \Pi_{GD}(f_t, Obj, Rel)$. The details of the function Π_{GD} are provided in Appendix.

Algorithm 1: Pivot Frame Retrieval (PFR)

Require: video frames \mathcal{F} , query Q , iterations P , stride ∇

Ensure: Pivot frames $\mathcal{F}_{pivot} = \{f_t\}_{t=1}^K$

```

1: Initialize:
2:  $\mathcal{S} \leftarrow \mathbf{0}^N$  ▷ Confidence scores
3:  $\mathcal{V} \leftarrow \emptyset$  ▷ Visited frames set
4:  $\{Obj, Des, Rel, Sem\} \leftarrow \text{LLM}(Q)$  ▷ Query Expansion
5: for  $p = 1$  to  $P$  do
6:    $\nabla_p \leftarrow \max\left(1, \frac{\nabla}{p}\right)$ 
7:    $\mathcal{F}_{samp}^p \leftarrow \text{AdaptiveResample}(\mathcal{F}, \mathcal{S}, \mathcal{V}, \nabla_p)$ 
8:   for  $f_t \in \mathcal{F}_{samp}^p$  do
9:      $s_t^{CLIP} \leftarrow \Pi_{CLIP}(f_t, Q, Des, Sem)$ 
10:     $s_t^{GD} \leftarrow \Pi_{GD}(f_t, Obj, Rel)$ 
11:     $\mathcal{S}_t \leftarrow (1 - \lambda)s_t^{CLIP} + \lambda s_t^{GD}$ 
12:     $\mathcal{S}_{[t-w, t+w]} \leftarrow \max\left(\mathcal{S}_{[t-w, t+w]}, \frac{\mathcal{S}_t}{1 + |i - t|}\right)$ 
13:   end for
14:    $\mathcal{V} \leftarrow \mathcal{V} \cup \mathcal{F}_{samp}^p$ 
15: end for
16: return  $\mathcal{F}_{pivot} \leftarrow \text{topk}(\mathcal{S} \odot \mathcal{F}, K)$ 

```

The final confidence score of this iteration is computed as a weighted sum of the CLIP and Grounding-DINO scores:

$$\mathcal{S}_t = (1 - \lambda) \cdot s_t^{CLIP} + \lambda \cdot s_t^{GD}. \quad (1)$$

The frames scored in the current iteration are put into the visited frame set \mathcal{V} .

Temporal Diffusion: To account for the temporal continuity of video content and improve frame resampling, we introduce a temporal score diffusion mechanism that propagates confidence scores across neighboring frames as:

$$\mathcal{S}_i = \max\left(\mathcal{S}_i, \frac{\mathcal{S}_t}{1 + |i - t|}\right), i \in [t - w, t + w] \quad (2)$$

This diffusion process helps capture temporally coherent segments relevant to the query.

Adaptive Resampling Based on the updated \mathcal{S} , we further design an adaptive and hybrid candidate sampling strategy for subsequent iterations that combines two types of set:

High-confidence Set: We select frames with higher scores from all unvisited frame set $\mathcal{U} = \{f_t \mid f_t \notin \mathcal{V}\}$ based on the distribution as:

$$\mathcal{H}_s = \text{TopK}(\mathcal{S} \odot \mathcal{U}, \frac{N}{2\nabla_p}) \quad (3)$$

Uncertainty Set: We calculate Shannon entropy based on the score distribution as:

$$\mathcal{E}_\gamma(s_i) = - \sum_{j=i-\gamma}^{i+\gamma} e_j \cdot \log(e_j), e_j = \frac{s_j}{\sum_{k=j-\gamma}^{j+\gamma} s_k} \quad (4)$$

, then the frames with high entropy are identified by:

$$\mathcal{H}_e = \{f_t \mid \mathcal{E}_\gamma(s_t) > \mu + 0.5\sigma\} \quad (5)$$

, where μ and σ are the mean and standard deviation of the entropy in \mathcal{C} .

The union candidate set for this iteration sampling is $\mathcal{C} = \mathcal{H}_s \cup \mathcal{H}_e$. Assume that there are $N_{\mathcal{C}}$ frames in \mathcal{C} . The frames \mathcal{F}_{samp}^p are sampled in the way as:

$$\mathcal{F}_{samp}^p = \mathcal{C}_{\text{multi}} \cup \mathcal{C}_{\text{rand}}, \quad (6)$$

$$\mathcal{C}_{\text{multi}} \sim \text{Multinomial}(\mathcal{S} \odot \mathcal{C}, (1 - \alpha)N_{\mathcal{C}}), \quad (7)$$

$$\mathcal{C}_{\text{rand}} \sim \text{Unif}(\text{Perm}(\mathcal{S} \odot \mathcal{C}, \alpha N_{\mathcal{C}})) \quad (8)$$

, where α balances the multinomial score-based importance sampling $\mathcal{C}_{\text{multi}}$ and the diverse random sampling $\mathcal{C}_{\text{rand}}$ to capture the full semantic content of the video and also to avoid falling into local optimal.

After P iterations, the K pivot frames are retrieved by $\mathcal{F}_{pivot} = \text{TopK}(\mathcal{S} \odot \mathcal{F}, K)$ and fed into the next module.

3.3 Pivot Token Retrieval

Pivot Token Retrieval extends the concept of semantic importance from frame-level to token-level granularity. In this module, we adaptively retrieve the pivot visual token within MLLM to maintain computational efficiency while preserving critical semantic information.

First, the retrieved pivot frames \mathcal{F}_{pivot} are processed by a Vision Encoder $\mathcal{G}(\cdot)$ and a Projector $\mathcal{P}(\cdot)$ to generate dense visual token representations: $\mathcal{T}_{vis} = \mathcal{G}(\mathcal{P}(\mathcal{F}_{pivot})) = \{\mathcal{T}_t\}_{t=1}^K$. Our objective is to retrieve the pivot token \mathcal{T}_{pivot} . To this end, we introduce two components: query-aware multi-layer attention scoring and adaptive token selection.

Query-aware Multi-Layer Attention Scoring We leverage the expanded semantic information from the LLM-augmented query to guide token selection across multiple transformer layers. First, the attention scores for layer l are computed as:

$$A_{cross}^l = \text{softmax}\left(\frac{q_{text}^l \cdot (k_{vis}^l)^T}{\sqrt{d}}\right) \quad (9)$$

, where $A_{cross}^l \in R^{h \times d \times d_q \times d_v}$, q_{text}^l denotes the query states derived from $\{Q, Des, Sem\}$ and k_{vis}^l denotes the key state derived from the visual tokens \mathcal{T}_{vis} . Then the token-level attention scores of each layer are aggregated at the query dimension by:

$$a^l = \sum_{d_q} A_{cross}^l. \quad (10)$$

This formulation captures how much attention each key token receives across all query positions, providing a comprehensive measure of its importance for the current layer's computations. The superscript l will be omitted for concision.

Adaptive Token Selection The simplest token selection strategy is to directly retain the Top-K tokens while evicting others. However, this approach ignores the continuity of visual tokens and may reduce accuracy. Another factor that matters is that attention scores across heads may exist disparities, which further result in independence between

Model	Params	Type	LongVideoBench Val	Long	VideoMME		Overall
Proprietary Models							
GPT4-V	-	training-based	59.1	53.5	-	-	59.9
GPT4-o	-	training-based	66.7	65.3	-	-	71.9
Gemini-1.5-Pro	-	training-based	64.0	67.4	-	-	75.0
Open-Source MLLMs							
VideoLLaVA(Lin et al. 2023)	7B	training-based	58.2	36.2	38.0	45.3	39.9
VITA-1.5(Fu et al. 2025)	7B	training-based	-	47.1	54.2	67.0	56.1
mPLUG-Owl3(Ye et al. 2024)	7B	training-based	52.1	50.1	57.7	70.0	59.3
VideoLLaMA3(Zhang et al. 2025)	7B	training-based	59.8	54.9	63.7	80.1	66.2
Oryx-1.5(Liu et al. 2024c)	7B	training-based	56.3	-	-	-	58.3
QuoTA(Luo et al. 2025)	7B	training-free	59.0	55.7	64.9	77.1	65.9
Video-XL(Shu et al. 2024)	7B	training-based	49.5	-	-	-	55.5
ViLaMP(Cheng et al. 2025)	7B	training-based	57.8	-	-	-	67.5
AdaReTaKe(Wang et al. 2025a)	7B	traning-free	62.6	58.3	-	-	67.7
AKS(Tang et al. 2025a)	7B	training-free	62.7	-	-	-	65.3
Kangaroo(Liu et al. 2024a)	8B	traning-based	54.8	-	-	-	46.6
NVILA(Liu et al. 2024d)	8B	training-based	57.7	54.8	62.2	75.7	64.2
ByteVideoLLM(Wang et al. 2024a)	14B	training-based	-	56.4	62.9	74.4	64.6
Qwen2-VL(Wang et al. 2024b)	7B	training-based	55.6	53.8	-	-	63.3
Qwen2-VL w/ APVR(ours)	7B	training-free	60.9	55.1	66.2	73.9	65.2
Qwen2.5-VL(Bai et al. 2025b)	7B	training-based	59.5	55.6	-	-	65.4
Qwen2.5-VL w/ APVR(ours)	7B	training-free	64.9	59.1	67.8	78.3	68.4

Table 1: Video understanding accuracy(%) on LongVideoBench and VideoMME. The proposed APVR is applied upon two baseline MLLMs. The Methods are divided into two categories: training-based and training-free. APVR based on Qwen2.5-VL achieved state-of-the-art results on both the two benchmarks.

heads. Thus, considering the continuity of visual tokens as well as the disparities across heads, we introduce an adaptive token selection strategy consisting of two components: dynamic chunk-wise selection and head-wise soft voting.

Dynamic Chunk-wise Selection: The long video understanding reaches the memory wall when prefilling the visual token. Thus, we perform token selection for the KV cache to reduce redundancy. Given a key or value cache to select, we first divide it into W chunks at the token dimension. Then, the base selection ratio of the chunk w is computed as:

$$\eta_w = \frac{\sum_w a}{\max(\{\sum_i a \mid i = 1, \dots, W\})} \quad (11)$$

The dynamic ratio of each chunk is calculated by:

$$\rho_w = \min(1.0, \sqrt{\frac{|\{j : a_j > 0.01 \cdot \max(a)\}|}{L_w}}) \quad (12)$$

, where L_w is the chunk length. The final selection ratio is determined by:

$$\gamma_w = \rho_w \cdot \eta_w \quad (13)$$

Head-wise Soft Voting Based on the ratio γ_w , we can select the pivot token in each chunk by:

$$\mathcal{Z}_w = \text{TopK}(a_w \odot \mathcal{T}_w, \gamma_w L_w) \quad (14)$$

This results may appear to be significant disparities in different attention heads. To figure out this, we introduce head-wise voting for final token selection:

$$\mathcal{Z}_w = \text{TopK}((\sum_{j=1}^h \text{softmax}(a_{w,j})) \odot \mathcal{T}_w, \gamma_w L_w) \quad (15)$$

, where the softmax function calculates the per-head scores and gives a soft voting via normalization and sum. Finally, we update the KV cache as the selected pivot token in each layer:

$$\mathcal{T}_{pivot} = \text{Concat}(\{\mathcal{Z}_w\}_{w=1}^W) \quad (16)$$

Finally, the selected pivot tokens will be fed into the MLLM to generate the final response.

4 Experiments

4.1 Experimental setup

Datasets We evaluate the performance of APVR in two popular benchmarks that contains hour-level videos: **LongVideoBench**(Wu et al. 2024). A benchmark for long-context video understanding, consisting of 3,763 videos with 6,678 annotated multiple-choice questions across 17 categories of referred reasoning questions. **VideoMME**(Fu et al. 2024). A multi-modal evaluation benchmark focused on fine-grained video understanding tasks requiring precise

Query: In the room on the screen, there is a man wearing green clothes with a beard. Behind him, there is a white cabinet and a wooden shelf. On the shelf, there is a black bag. What did the man in the video do upon entering the scene?

Expanded Semantic Information:

"key_objects": [{"man", "white cabinet", "wooden shelf", "black bag"}]
 "cue_objects": [{"green clothes", "beard", "right hand", "left hand"}]
 "relations": [{"man", "Attribute", "green clothes"}, {"man", "Spatial", "black bag"}]
 "descriptions": [{"beard": "facial hair feature on man"}]
 "semantics": [{"right hand and left hand are body parts used for touching or carrying objects"}]

Retrieved Pivot Frames:



Qwen2.5-VL:
B. Touched his beard with his right hand

Qwen2.5-VL w/ APVR:
D. Touched his beard with his left hand

Query: In a white room, a man wearing a dark blue jacket is speaking on screen. There is a black microphone in front of him, he has dark skin, and he is sporting a beard. A black map is hanging on the wall behind him, there is a whiteboard on the left side of the screen, and on the right side, there is another wall with a black-bordered paper on it. What changes occur to this man's position on the screen when the 'Quiz Time 3' title, featuring many horizontal grids with black letters, appears?

Expanded Semantic Information:

"key_objects": [{"man", "microphone", "map"}]
 "cue_objects": [{"whiteboard", "black-bordered paper", "Quiz Time 3 title"}]
 "relations": [{"man", "Spatial", "microphone"}, {"man", "Spatial", "Quiz Time 3 title"}, {"man", "Spatial", "map"}]
 "descriptions": [{"microphone": "device for amplifying sound; positioned in front of man"}]
 "semantics": [{"titles may reposition subjects to maintain visibility"}]

Retrieved Pivot Frames:



Qwen2.5-VL:
C. The man's position on the screen shifts to the bottom-left corner.

Qwen2.5-VL w/ APVR:
D. The man's position on the screen shifts to the bottom-right corner.

Query: On the surface of the sink are a toothbrush and toothpaste. Reflected in the glass above the sink is a man wearing a white hat and a white short-sleeved shirt, holding a camera. What changes when this man appears in the driver's seat?

Expanded Semantic Information:

"key_objects": [{"man", "white hat", "white short-sleeved shirt", "camera"}]
 "cue_objects": [{"sink", "toothbrush", "toothpaste", "driver's seat"}]
 "relations": [{"man", "Attribute", "white hat"}, {"man", "Attribute", "white short-sleeved shirt"}, {"man", "Spatial", "camera"}]
 "descriptions": [{"white hat": "headwear worn by the man; protective or decorative headgear"}]
 "semantics": [{"driver's seat implies a vehicle context"}]

Retrieved Pivot Frames:



Qwen2.5-VL:
E. He changed to a gray long-sleeved coat

Qwen2.5-VL w/ APVR:
B. He changed to a black long-sleeved coat

Query: The video shows the interior of a museum with two white light fixtures. Many white cabinets containing different artifacts are placed on the dark-colored floor. On the right side of the screen, a woman is sitting in a room illuminated by white lights, shown in a small video frame. What material is the protective cover placed over the artifacts on the cabinet made of?

Expanded Semantic Information:

"key_objects": [{"white light fixtures", "white cabinets", "artifacts"}]
 "cue_objects": [{"protective cover", "dark-colored floor", "woman in illuminated room"}]
 "relations": [{"white cabinets", "Spatial", "protective cover"}]
 "descriptions": [{"protective cover": "transparent material; artifact protection device"}]
 "semantics": [{"protective covers are often made of glass or acrylic for artifact preservation", "glass is commonly used in museums due to its transparency and durability"}]

Retrieved Pivot Frames:



Qwen2.5-VL:
E. Acrylic

Qwen2.5-VL w/ APVR:
C. Glass

Figure 3: Qualitative Comparison of APVR with the baseline MLLM. The expanded query is significant complementary for pivot information retrieval. The number and score of the pivot frame is drawn in the left-top with green and red text, respectively. Yellow stars indicate the key frame for correct response. Green answer represents correct while red one represents wrong.

visual-textual alignment and detailed semantic comprehension. It comprises 900 videos totaling 256 hours, with 2,700 manually labeled complex multiple-choice question-answer pairs across 30 subfields. To highlight the importance of the pivot information retrieval for visual understanding, we do not use video subtitles for the two benchmarks.

Implementation Details We integrate APVR with two baseline MLLMs, namely, Qwen2-VL-7B (Wang et al. 2024b) and Qwen2.5-VL-7B (Bai et al. 2025b). The MLLMs process a prompt involving the question, retrieved pivot video frames, and the multi-choice answer options to generate responses. We first densely extracted the raw frames from video with $fps = 2$. Then, the sampled frames are iteratively scored using two basic visual models: CLIP (Radford et al. 2021) with ViT-B-16 (Dosovitskiy et al. 2020) backbone, and Grounding-DINO (Liu et al. 2024b) with Swin-T (Liu et al. 2021) backbone, based on the expanded semantic information generated by LLM. All evaluations are conducted on 8 NVIDIA A800 GPUs with 80GB memory, using LMMs-Eval (Zhang et al. 2024a) framework. Under the above setup, our APVR enables processing of up to 1024 frames, compared to the baseline 7B model’s capacity of 256 frames under optimal MLLM configurations.

4.2 Comparison to the State-of-the-Art

Quantitative results We first compare the accuracy of video question answering between APVR with recent

training-based or training-free methods. All results are summarized in Table 1. Upon the Qwen2-VL baseline, APVR improves the overall accuracy by 9.5% and 3.0% in LongVideoBench and VideoMME, respectively. Upon a stronger baseline Qwen2.5-VL, our APVR also improves the overall accuracy by 8.3% in LongVideoBench and 4.6% in VideoMME, respectively. Notably, APVR based on Qwen2.5-VL reaches 64.9% accuracy in LongVideoBench, which is higher than the powerful proprietary models such as GPT4-V and Gemini-1.5-Pro. The overall performance of APVR also surpasses other training-based and training-free methods with larger parameter scales such as 8B and 14B. Another notable result is that our APVR reaches highest accuracy on long and medium video samples of VideoMME, confirming its unique capability to preserve critical spatio-temporal information in extended sequences.

Qualitative results Fig. 3 presents representative qualitative results on hour-level video understanding, comparing our APVR framework with the baseline Qwen2.5-VL across four challenging samples. The results clearly demonstrate the unique advantages of APVR in both the semantic expansion and the subsequent retrieval process.

Firstly, the semantic information expansion module in APVR significantly enriches the original query, providing the downstream retrieval process with comprehensive object, attribute, and relational cues that are otherwise missing when using only the raw query. This richer semantic context

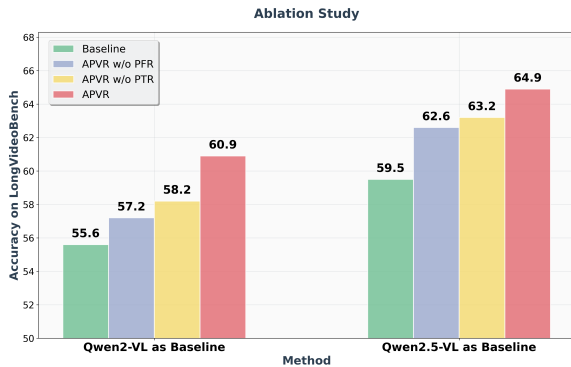


Figure 4: The result of ablation study on LongVideoBench for the two designed components: PFR and PTR.

enables the retrieval module to more accurately identify and prioritize frames that are truly relevant to the query intent.

Secondly, we observe that the pivot frames selected by APVR are highly correlated with both the query and the expanded semantic information, effectively filtering out irrelevant or redundant content. In long videos, there often exist temporally adjacent frames that are visually similar and all somewhat related to the query. If only a very limited number of frames are selected, it is easy to miss critical moments; conversely, retaining an excessive number of frames (e.g., 1024 frames) would cause out-of-memory (OOM) errors. APVR overcomes this dilemma by PFR and PTR and distills the most informative visual information within sufficient pivot frames. As a result, APVR empowers MLLM to efficiently comprehend long-form video content, providing accurate and detailed answers even in scenarios where baselines fail or generate hallucinations.

4.3 Ablation Studies

Ablation studies on PFR and PTR To systematically validate the effectiveness of the proposed dual-granularity retrieval strategy, we conduct ablation studies on the two core components of APVR: Pivot Frame Retrieval (PFR) and Pivot Token Retrieval (PTR), using the LongVideoBench benchmark. The results, shown in Fig. 4, consistently demonstrate that removing either PFR or PTR leads to a notable decline in accuracy across both baseline MLLMs. Without PFR, the system loses its ability to precisely localize query-relevant frames, resulting in performance degradation due to the inclusion of irrelevant or redundant content. Without PTR, the model is less able to compress visual tokens and focus on the most informative visual details, leading to processing maximum to only 256 frames and reduced answer quality. These findings strongly support the necessity and rationality of our dual-granularity pivot information retrieval design.

Ablation studies on other hyper-parameters We further conduct a comprehensive analysis of key hyper-parameters that influence the performance of APVR. First, we examine the impact of the number of retrieved pivot frames K and the weighting parameter λ that balances the contributions of the two visual models in frame scoring. As summarized

K	Long	Average	λ	Long	Average
1024	58.3	64.9	0.1	57.4	64.2
256	56.4	63.1	0.2	57.8	64.5
128	53.0	61.1	0.5	58.3	64.9
64	49.8	58.6	0.8	58.0	64.8
32	45.4	54.3	0.9	58.9	64.5

Table 2: Ablations of retained frame number and weight for scoring models.

P	∇	Long	Medium	Short	Average
3	2	56.4	62.1	77.3	62.9
3	4	58.3	65.8	77.3	64.9
3	8	55.1	64.6	77.3	63.1
2	4	56.0	66.0	77.3	63.9
4	4	58.0	65.8	77.3	64.7
5	4	58.5	64.5	77.3	64.5

Table 3: Ablations of iteration number and the initial sample stride.

in Table 2, increasing the number of retained frames generally improves performance, especially on long videos, by reducing the risk of missing relevant segments. For the model weighting parameter λ , we observe that optimal results are achieved by striking a balance between CLIP-based semantic similarity and Grounding-DINO-based object detection, confirming the complementarity of these two perspectives.

Second, we analyze the effect of core retrieval hyper-parameters, specifically the number of retrieval iterations p and the initial sampling stride ∇ . As shown in Table 3, the best performance is observed when $P = 3$ and $\nabla = 4$, indicating that a moderate number of adaptive iterations and a balanced initial sampling density allow the system to progressively refine frame selection without causing overfitting or excessive computational cost. Deviating from these settings leads to decreased accuracy, highlighting the importance of carefully tuning the retrieval process to maintain a balance between sampling and distribution update.

5 Conclusion

We propose APVR, a training-free framework that overcomes the memory wall in hour-level video understanding via adaptive, hierarchical visual information retrieval. By integrating Pivot Frame Retrieval and Pivot Token Retrieval, APVR enables efficient and accurate processing of long videos without sacrificing semantic detail. Extensive experiments on standard benchmarks demonstrate that APVR delivers state-of-the-art results among training-free and training-based methods. Its plug-and-play design allows seamless integration with existing MLLM systems, eliminating the need for costly retraining. Our results establish retrieval-based optimization as a practical and scalable solution for long-form video comprehension.

References

- Ataallah, K.; Shen, X.; Abdelrahman, E.; Sleiman, E.; Zhuge, M.; Ding, J.; Zhu, D.; Schmidhuber, J.; and Elhoseiny, M. 2024. Goldfish: Vision-language understanding of arbitrarily long videos. In *European Conference on Computer Vision*, 251–267. Springer.
- Bai, S.; Chen, K.; Liu, X.; Wang, J.; Ge, W.; Song, S.; Dang, K.; Wang, P.; Wang, S.; Tang, J.; et al. 2025a. Qwen2. 5-vl technical report. *arXiv preprint arXiv:2502.13923*.
- Bai, S.; Chen, K.; Liu, X.; Wang, J.; Ge, W.; Song, S.; Dang, K.; Wang, P.; Wang, S.; Tang, J.; et al. 2025b. Qwen2. 5-vl technical report. *arXiv preprint arXiv:2502.13923*.
- Chen, Y.; Xue, F.; Li, D.; Hu, Q.; Zhu, L.; Li, X.; Fang, Y.; Tang, H.; Yang, S.; Liu, Z.; et al. 2024. Longvila: Scaling long-context visual language models for long videos. *arXiv preprint arXiv:2408.10188*.
- Cheng, C.; Guan, J.; Wu, W.; and Yan, R. 2025. Scaling Video-Language Models to 10K Frames via Hierarchical Differential Distillation. *arXiv preprint arXiv:2504.02438*.
- Dosovitskiy, A.; Beyer, L.; Kolesnikov, A.; Weissenborn, D.; Zhai, X.; Unterthiner, T.; Dehghani, M.; Minderer, M.; Heigold, G.; Gelly, S.; et al. 2020. An image is worth 16x16 words: Transformers for image recognition at scale. *arXiv preprint arXiv:2010.11929*.
- Fu, C.; Dai, Y.; Luo, Y.; Li, L.; Ren, S.; Zhang, R.; Wang, Z.; Zhou, C.; Shen, Y.; Zhang, M.; et al. 2024. Videomme: The first-ever comprehensive evaluation benchmark of multi-modal llms in video analysis. *arXiv preprint arXiv:2405.21075*.
- Fu, C.; Lin, H.; Wang, X.; Zhang, Y.-F.; Shen, Y.; Liu, X.; Cao, H.; Long, Z.; Gao, H.; Li, K.; et al. 2025. Vita-1.5: Towards gpt-4o level real-time vision and speech interaction. *arXiv preprint arXiv:2501.01957*.
- Guo, W.; Chen, Z.; Wang, S.; He, J.; Xu, Y.; Ye, J.; Sun, Y.; and Xiong, H. 2025. Logic-in-Frames: Dynamic Keyframe Search via Visual Semantic-Logical Verification for Long Video Understanding. *arXiv preprint arXiv:2503.13139*.
- Li, K.; Li, X.; Wang, Y.; He, Y.; Wang, Y.; Wang, L.; and Qiao, Y. 2024a. Videomamba: State space model for efficient video understanding. In *European Conference on Computer Vision*, 237–255. Springer.
- Li, X.; Wang, Y.; Yu, J.; Zeng, X.; Zhu, Y.; Huang, H.; Gao, J.; Li, K.; He, Y.; Wang, C.; et al. 2024b. Videochat-flash: Hierarchical compression for long-context video modeling. *arXiv preprint arXiv:2501.00574*.
- Lin, B.; Ye, Y.; Zhu, B.; Cui, J.; Ning, M.; Jin, P.; and Yuan, L. 2023. Video-llava: Learning united visual representation by alignment before projection. *arXiv preprint arXiv:2311.10122*.
- Liu, J.; Wang, Y.; Ma, H.; Wu, X.; Ma, X.; Wei, X.; Jiao, J.; Wu, E.; and Hu, J. 2024a. Kangaroo: A powerful video-language model supporting long-context video input. *arXiv preprint arXiv:2408.15542*.
- Liu, S.; Zeng, Z.; Ren, T.; Li, F.; Zhang, H.; Yang, J.; Jiang, Q.; Li, C.; Yang, J.; Su, H.; et al. 2024b. Grounding dino: Marrying dino with grounded pre-training for open-set object detection. In *European Conference on Computer Vision*, 38–55. Springer.
- Liu, X.; Shu, Y.; Liu, Z.; Li, A.; Tian, Y.; and Zhao, B. 2025a. Video-XL-Pro: Reconstructive Token Compression for Extremely Long Video Understanding. *arXiv preprint arXiv:2503.18478*.
- Liu, Y.; Lin, K. Q.; Chen, C. W.; and Shou, M. Z. 2025b. VideoMind: A Chain-of-LoRA Agent for Long Video Reasoning. *arXiv preprint arXiv:2503.13444*.
- Liu, Z.; Dong, Y.; Liu, Z.; Hu, W.; Lu, J.; and Rao, Y. 2024c. Oryx mllm: On-demand spatial-temporal understanding at arbitrary resolution. *arXiv preprint arXiv:2409.12961*.
- Liu, Z.; Lin, Y.; Cao, Y.; Hu, H.; Wei, Y.; Zhang, Z.; Lin, S.; and Guo, B. 2021. Swin transformer: Hierarchical vision transformer using shifted windows. In *Proceedings of the IEEE/CVF international conference on computer vision*, 10012–10022.
- Liu, Z.; Zhu, L.; Shi, B.; Zhang, Z.; Lou, Y.; Yang, S.; Xi, H.; Cao, S.; Gu, Y.; Li, D.; et al. 2024d. NVILA: Efficient frontier visual language models. *arXiv preprint arXiv:2412.04468*.
- Luo, Y.; Chen, W.; Zheng, X.; Huang, W.; Yin, S.; Lin, H.; Fu, C.; Huang, J.; Ji, J.; Luo, J.; et al. 2025. QuoTA: Query-oriented Token Assignment via CoT Query Decouple for Long Video Comprehension. *arXiv preprint arXiv:2503.08689*.
- Park, J.; Ranasinghe, K.; Kahatapitiya, K.; Ryu, W.; Kim, D.; and Ryoo, M. S. 2024. Too many frames, not all useful: Efficient strategies for long-form video qa. *arXiv preprint arXiv:2406.09396*.
- Radford, A.; Kim, J. W.; Hallacy, C.; Ramesh, A.; Goh, G.; Agarwal, S.; Sastry, G.; Askell, A.; Mishkin, P.; Clark, J.; et al. 2021. Learning transferable visual models from natural language supervision. In *International conference on machine learning*, 8748–8763. PmLR.
- Shen, X.; Xiong, Y.; Zhao, C.; Wu, L.; Chen, J.; Zhu, C.; Liu, Z.; Xiao, F.; Varadarajan, B.; Bordes, F.; et al. 2024. Longvu: Spatiotemporal adaptive compression for long video-language understanding. *arXiv preprint arXiv:2410.17434*.
- Shen, Y.; Fu, C.; Dong, S.; Wang, X.; Chen, P.; Zhang, M.; Cao, H.; Li, K.; Zheng, X.; Zhang, Y.; et al. 2025. Long-VITA: Scaling Large Multi-modal Models to 1 Million Tokens with Leading Short-Context Accuracy. *arXiv preprint arXiv:2502.05177*.
- Shu, Y.; Liu, Z.; Zhang, P.; Qin, M.; Zhou, J.; Liang, Z.; Huang, T.; and Zhao, B. 2024. Video-xl: Extra-long vision language model for hour-scale video understanding. *arXiv preprint arXiv:2409.14485*.
- Song, E.; Chai, W.; Wang, G.; Zhang, Y.; Zhou, H.; Wu, F.; Chi, H.; Guo, X.; Ye, T.; Zhang, Y.; et al. 2024. Moviechat: From dense token to sparse memory for long video understanding. In *Proceedings of the IEEE/CVF Conference on Computer Vision and Pattern Recognition*, 18221–18232.

Su, J.; Ahmed, M.; Lu, Y.; Pan, S.; Bo, W.; and Liu, Y. 2024. Roformer: Enhanced transformer with rotary position embedding. *Neurocomputing*, 568: 127063.

Tang, X.; Qiu, J.; Xie, L.; Tian, Y.; Jiao, J.; and Ye, Q. 2025a. Adaptive Keyframe Sampling for Long Video Understanding. *arXiv preprint arXiv:2502.21271*.

Tang, X.; Qiu, J.; Xie, L.; Tian, Y.; Jiao, J.; and Ye, Q. 2025b. Adaptive Keyframe Sampling for Long Video Understanding. *arXiv preprint arXiv:2502.21271*.

Wang, H.; Nie, Y.; Ye, Y.; GuanYu, D.; Wang, Y.; Li, S.; Yu, H.; Lu, J.; and Huang, C. 2024a. Dynamic-VLM: Simple Dynamic Visual Token Compression for VideoLLM. *arXiv preprint arXiv:2412.09530*.

Wang, P.; Bai, S.; Tan, S.; Wang, S.; Fan, Z.; Bai, J.; Chen, K.; Liu, X.; Wang, J.; Ge, W.; et al. 2024b. Qwen2-vl: Enhancing vision-language model’s perception of the world at any resolution. *arXiv preprint arXiv:2409.12191*.

Wang, X.; Si, Q.; Wu, J.; Zhu, S.; Cao, L.; and Nie, L. 2025a. AdaRETAKE: Adaptive Redundancy Reduction to Perceive Longer for Video-language Understanding. *arXiv preprint arXiv:2503.12559*.

Wang, X.; Zhang, Y.; Zohar, O.; and Yeung-Levy, S. 2024c. Videoagent: Long-form video understanding with large language model as agent. In *European Conference on Computer Vision*, 58–76. Springer.

Wang, Y.; Li, X.; Yan, Z.; He, Y.; Yu, J.; Zeng, X.; Wang, C.; Ma, C.; Huang, H.; Gao, J.; et al. 2025b. InternVideo2.5: Empowering Video MLLMs with Long and Rich Context Modeling. *arXiv preprint arXiv:2501.12386*.

Wei, X.; Liu, X.; Zang, Y.; Dong, X.; Zhang, P.; Cao, Y.; Tong, J.; Duan, H.; Guo, Q.; Wang, J.; et al. 2025. VideoRoPE: What Makes for Good Video Rotary Position Embedding? *arXiv preprint arXiv:2502.05173*.

Wu, H.; Li, D.; Chen, B.; and Li, J. 2024. Longvideobench: A benchmark for long-context interleaved video-language understanding. *Advances in Neural Information Processing Systems*, 37: 28828–28857.

Ye, J.; Wang, Z.; Sun, H.; Chandrasegaran, K.; Durante, Z.; Eyzaguirre, C.; Bisk, Y.; Niebles, J. C.; Adeli, E.; Fei-Fei, L.; et al. 2025. Re-thinking Temporal Search for Long-Form Video Understanding. *arXiv preprint arXiv:2504.02259*.

Ye, J.; Xu, H.; Liu, H.; Hu, A.; Yan, M.; Qian, Q.; Zhang, J.; Huang, F.; and Zhou, J. 2024. mplug-owl3: Towards long image-sequence understanding in multi-modal large language models. *arXiv preprint arXiv:2408.04840*.

Zhang, B.; Li, K.; Cheng, Z.; Hu, Z.; Yuan, Y.; Chen, G.; Leng, S.; Jiang, Y.; Zhang, H.; Li, X.; et al. 2025. VideoLLaMA 3: Frontier Multimodal Foundation Models for Image and Video Understanding. *arXiv preprint arXiv:2501.13106*.

Zhang, K.; Li, B.; Zhang, P.; Pu, F.; Cahyono, J. A.; Hu, K.; Liu, S.; Zhang, Y.; Yang, J.; Li, C.; et al. 2024a. Lmms-eval: Reality check on the evaluation of large multimodal models. *arXiv preprint arXiv:2407.12772*.

Zhang, P.; Zhang, K.; Li, B.; Zeng, G.; Yang, J.; Zhang, Y.; Wang, Z.; Tan, H.; Li, C.; and Liu, Z. 2024b. Long

context transfer from language to vision. *arXiv preprint arXiv:2406.16852*.

6 Appendix

6.1 Prompt Template for Query Expansion

The prompt in Fig. 5 was used to interact with the language model for semantic information expansion.

6.2 The Details of Spatio-semantic Confidence Scoring

Semantic Scoring For each of the sampled frames $\mathcal{F}_{samp} = \{f_t\}_{t=1}^{N_s}$, we encode it using the CLIP image encoder $\phi_I(\cdot)$:

$$v_t = \frac{\phi_I(f_t)}{\|\phi_I(f_t)\|_2}. \quad (17)$$

The query as well as the expanded description and semantics are aggregated and encoded using the CLIP text encoder $\phi_T(\cdot)$:

$$t_{agg} = \sum_e \frac{\phi_T(e)}{\|\phi_T(e)\|_2}, e \in \{Q, Des, Sem\}. \quad (18)$$

The CLIP similarity score for frame f_t is then calculated as:

$$s_t^{CLIP} = softmax(\tau \cdot v_t \cdot t_{agg}) \quad (19)$$

, where τ is a temperature parameter set to 100 to sharpen the score distribution.

Spatial Scoring To enhance the retrieval precision with key/cue objects along with their relations, we first employ Grounding-DINO to identify extracted objects:

$$\mathcal{B}_t, \mathcal{L}_t = \Psi_{GD}(f_t, O_k \cup O_c) \quad (20)$$

, where $\Psi(\cdot)$ is the Grounding-DINO model that returns bounding boxes \mathcal{B}_t and corresponding confidence logits \mathcal{L}_t for frame f_t . The score of detection is then computed as:

$$s_t^o = softmax(max(\mathcal{L}_t)). \quad (21)$$

To further model the logic relations among objects in the same or different frames to enhance the detection results, we update the score by adding corresponding frame score if there are satisfied relation triplets in this frame as follows:

$$s_t^{GD} = s_t^o + \sum_r (\omega_r \cdot s_r) \quad (22)$$

, where r is exactly one of spatial/time/attribute/causal and ω_r is the corresponding weight to control the contribution of each type of relation.

Query Expansion Prompt Example

Analyze the following video understanding question:

Question: <Question>; Options: <Options>

Step 1: Key Object Identification

- Extract 3-5 core objects detectable by computer vision
- Use Grounding dino compatible noun phrases (e.g., “person”, “mic”)
- Format: Key Objects: obj1, obj2, obj3

Step 2: Contextual Cues

- List 2-4 scene elements that help locate key objects based on options provided
- Use detectable items (avoid abstract concepts)
- Format: Cue Objects: cue1, cue2, cue3

Step 3: Relationship Triplets

- Relationship types:
 - Spatial: Objects must appear in the same frame
 - Attribute: Color/size/material descriptions (e.g., “red clothes”, “large”)
 - Time: Appear in different frames within a few seconds
 - Causal: There is a temporal order between the objects
- Format of Relations: (object, relation type, object), relation type should be exactly one of spatial/attribute/time/-causal

Step 4: Description Augmentation

- List 1-3 descriptions based on knowledge graph augmentation for each object
- Entity descriptions (e.g., “mic is a device for amplifying sound”)
- Hypernym concepts (e.g., “dog is a kind of animal”)
- Format: Description: (object: des1; des2)

Step 5: Semantics Augmentation

- List 2-5 Semantics information of query and options based on knowledge graph (e.g., “leash often appears with dog”)
- Format: Semantics: semantic1; semantic2

Output Rules

1. One line each for Key Objects/Cue Objects/Relation/Des/Sem starting with exact prefixes
2. Separate items with comma except for triplets where items are separated by semicolon
3. Never use markdown or natural language explanations
4. If you cannot identify any key objects or cue objects from the video provided, please just identify the possible key or cue objects from the question and options provided

Below is an example of the procedure:

Question: For “When does the person in red clothes appear with the dog?”

Response:

Key Objects: person, dog, red clothes
Cue Objects: grassy area, leash, fence
Rel: (person; attribute; red clothes), (person; spatial; dog)
Des: (red clothes: description1), (dog: description2)
Sem: semantic1; semantic2

Format your response EXACTLY like this in Five lines:

Key Objects: object1, object2
Cue Objects: object3, object4
Rel: (object1; relation type1; object2), (object3; relation type2; object4), ...
Des: (object1: description1; description2), (object2: description1; description2), ...
Sem: semantic1; semantic2, ...

Figure 5: The Prompt Template for Query Expansion.